



PERGAMON

Scripta Materialia 45 (2001) 807–814



www.elsevier.com/locate/scriptamat

Lattice rotation of the cube orientation to the β fiber during cold rolling of AA 5052 aluminum alloy

W.C. Liu^{a*}, C.-S. Man^b, and J.G. Morris^a

^a*Light Metals Research Laboratory, Department of Chemical and Materials Engineering, University of Kentucky, 177 Anderson Hall, Lexington, KY 40506, USA*

^b*Department of Mathematics, University of Kentucky, 715 Patterson Office Tower, Lexington, KY 40506, USA*

Received 21 March 2001; accepted 10 May 2001

Abstract

The hot bands and annealed hot bands of AA 5052 aluminum alloy were cold rolled to different reductions ranging from 0% to 92%. The ODFs of cold rolled samples were determined by X-ray diffraction. The rotation path of the cube orientation to the β fiber was determined based on the variation in the orientation distribution function with reduction, and the stability of orientations on the β fiber was discussed. © 2001 Acta Materialia Inc. Published by Elsevier Science Ltd. All rights reserved.

Keywords: Aluminium; Cold rolling; Texture; X-ray diffraction; Lattice rotation

Introduction

The formation of texture is due to lattice rotation during deformation. Many experimental and theoretical studies have been carried out on lattice rotation in single crystals and polycrystalline materials, especially in cube oriented single crystals [1–6].

Dillamore and Katoh [1] predicated that an orientation which was deviated a little from the cube orientation moved first the cube orientation by a rotation about the rolling direction (RD), and then separated into two components by large lattice rotations about the normal direction (ND). Akef and Driver [2] analyzed the lattice rotation of cube-oriented fcc crystals during plane strain compression. Texture analyses of single crystals deformed in plane strain compression to strains in the range 0.25–1.5 revealed the extensive lattice rotation about the transverse direction (TD). Different regions of the crystals rotated in opposite directions about TD, leading to splitting of the original

* Corresponding author.

E-mail address: wenchangliu@hotmail.com (W.C. Liu).

crystal into complementary texture components. Engler et al. [3] studied the texture evolution during rolling of cube-oriented Al–Cu single crystals. At low degrees of rolling up to about 63% thickness reduction the initial cube orientation was retained but showed a strong orientation scatter. At 78% reduction the single cube orientation was decomposed by diverging \pm RD rotations into two different components, while at 95% reduction the four symmetrical variants of the rolling texture S orientation were distinguished.

The crystallite orientations in a cube-oriented Al single crystal deformed by rolling [4] and plane strain compression [5] have been analyzed using TEM diffraction methods. Liu et al. [5] found that the crystal rotations were predominantly about TD, but non-TD rotations also occurred in the cube-oriented crystal. EBSP measurements of crystallite orientations revealed that coarse deformation banding started by rotations about TD, and then further rotation continued about TD but also developed about RD [6].

The simulation of texture development during cold rolling has been carried out by using the full or relaxed constraints of the Taylor–Bishop–Hill model [7], a strain rate sensitivity model [8] and a modified pencil glide theory [9]. Hirsch and Lücke [7] calculated the paths of the (10, 0.1, 89.9) orientation by using the Taylor theory of polycrystalline plasticity under conditions of full and relaxed constraints. For the group I models in which the $\varepsilon_{TD/RD}$ shear is 0, the orientation moves at first towards the α fiber. They leave the α fiber before reaching the B orientation and move directly towards their final stable positions at the D or C orientation. For the group II models in which the $\varepsilon_{TD/RD}$ shear is relaxed, the orientation move towards the α fiber, and no further orientation change takes place after the α fiber is reached. For the N model (Sachs theory) the rotation path is through the G orientation to the B orientation, and the B orientation is the stable end position. Zhou et al. [8] predicted using a rate-sensitive crystal plasticity model that the orientation (1, 1, 89) first rotated to the α fiber during rolling, then along the α fiber to the β fiber, and finally is stabilized at the D or C orientation. Masui [9] simulated the fcc rolling texture by a modified pencil glide theory. The results showed that the cube orientation moved to the G orientation and finally to the B orientation during rolling. In the present work, AA 5052 aluminum alloy hot bands were annealed at 371°C for 3 h to obtain a polycrystalline aluminum alloy with the cube texture, and then cold rolled to different reductions. The rotation paths of the cube orientation during rolling were determined based on the variation in the orientation distribution function with reduction. At the same time AA 5052 aluminum alloy hot bands with the β fiber rolling texture were also cold rolled to different reductions in order to determine the stability of orientations on the β fiber during rolling.

Experimental

The material used in the present investigation is AA 5052 aluminum alloy. The chemical composition of the alloy is (in wt.%): 96.9 Al, 0.115 Si, 0.372 Fe, 0.055 Mn, 2.363 Mg, and 0.191 Cr. The as-received material was strip cast hot bands, which were produced using standard industrial practices. The hot bands with a thickness of 2.1 mm

were annealed at 371°C for 3 h followed by air cooling. The hot bands before and after annealing at 371°C were cold rolled to different reductions ranging from 0% to 92%.

Texture measurements were performed at one fourth-thickness of the sheets. The (1 1 1), (2 0 0), (2 2 0), and (3 1 1) pole figures were measured up to a maximum tilt angle of 75° by the Schulz back-reflection method using CuK_α radiation. The intensities of pole figures were corrected for defocusing and absorption with a powder sample of commercial purity aluminum. The ODFs were calculated from the incomplete pole figures and presented as plots of constant ϕ_2 sections with isointensity contours in Euler space defined by the Euler angles ϕ_1 , ϕ , and ϕ_2 .

Results

Path of crystal rotation from the cube orientation to the β fiber during cold rolling

Fig. 1 shows the ODFs of samples cold rolled to different reductions after annealing at 371°C for 3 h. When the hot band is annealed at 371°C for 3 h, the texture of AA 5052 alloy is mainly composed of the cube component and the Goss component, as shown in Fig. 1(a). Fig. 2(a) shows the position of the cube component relative to the ϕ_1 , ϕ , ϕ_2 coordinate system. It is noted that the cube component concentrates on the eight corners of the cube and along the fiber running from 90°, 0° and 0° to 0°, 0° and 90° in the subset of Euler space in which $0 < \phi_1, \phi, \phi_2 < \pi/2$.

During cold rolling the cube component is gradually converted into the β fiber component. The texture is mainly composed of the β fiber when the cold rolling reduction reaches 92%. The position of the β fiber is also drawn in Fig. 2(a) based on the symmetry of orientations on the β fiber in the part of Euler space given by $-\pi/2 < \phi_1, \phi, \phi_2 < \pi/2$. It is noted that the β fiber appears as a closed loop in the full Euler space.

The path of the lattice rotation from the cube orientation to the β fiber can be determined based on the variation in the three-dimensional orientation distribution

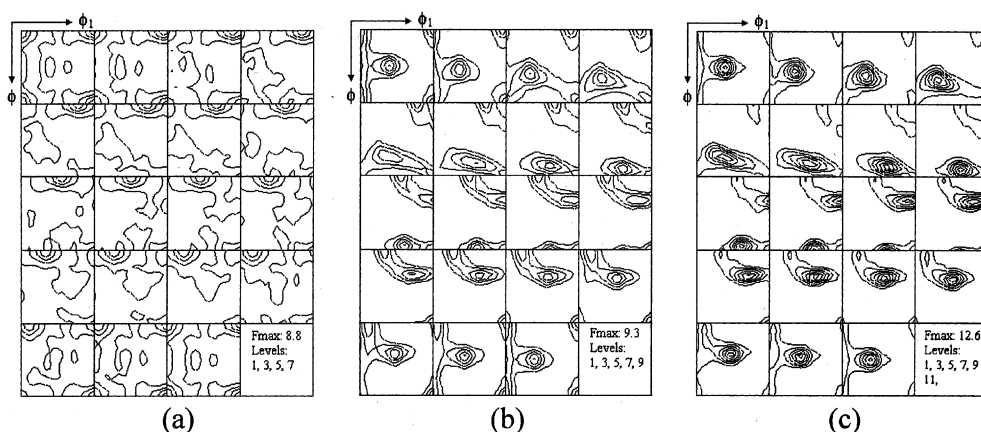


Fig. 1. ODFs of hot band samples cold rolled to reductions of (a) 0%, (b) 48.8%, and (c) 74.4% after annealing at 371°C for 3 h.

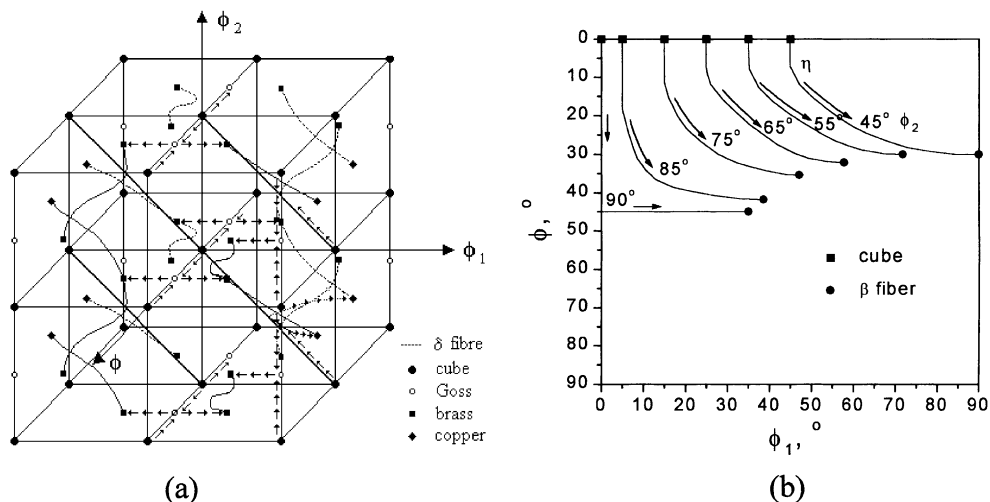


Fig. 2. Schematic presentation of the lattice rotation paths from the cube orientation to the β fiber (a) in Euler space and (b) for specific values of Euler angle ϕ_2 from 45° to 90°.

function with cold rolling reduction. Fig. 2(a) shows the orientation arrow chart which indicates the lattice rotation paths from the cube orientation to the β fiber during rolling. It is noted that the rotation path from the cube orientation to the β fiber can be divided into two cases. The first case is that the cube orientation is rotated to an orientation of the B component through the Goss orientation. Because of the intrinsic non-uniqueness in the representation of orientation of a cubic crystal in the Euler space, this rotation is shown in multiple paths in Fig. 2(a): the points (0, 0, 0) and (0, 90, 0) which represents the cube orientation, are rotated to the B (35, 45, 0) orientation through the G (0, 45, 0) orientation, while the representative points (0, 0, 90) and (0, 90, 90) of the cube orientation are rotated to the B (35, 45, 90) orientation through the G (0, 45, 90) orientation, and the points (90, 90, 0) and (90, 90, 90) move to the B (55, 90, 45) through the G (90, 90, 45) orientation. In the second case the cube orientation, as represented by the points along the line segment joining (45, 0, 45) and (0, 0, 90) in the Euler space, are directly rotated to the β fiber between the D (90, 30, 45) orientation and the B (35, 45, 90) orientation. Their rotation paths for a particular angle ϕ_2 from 45° to 90° are shown in Fig. 2(b). According to the paths of the lattice rotation from the cube orientation to the β fiber, it is noted that the β fiber running from the B orientation at 35°, 45°, 0° to the C orientation at 39°, 66°, 27° is not symmetrically equivalent to that from the B orientation at 35°, 45°, 90° to the D orientation at 90°, 30°, 45°.

Formation and dissolution of orientation fibers

It is found from the ODFs in Fig. 1 that the distribution of intensities at the plane of $\phi_2 = 0^\circ$ is the same as those at the planes of $\phi_2 = 90^\circ$ and $\phi = 90^\circ$. Fig. 3(a) and (b) show typical intensities of the ODF $f(g)$ along the line of $\phi_1 = 0^\circ$ and $\phi = 45^\circ$ at the plane of $\phi_2 = 0^\circ$ for different cold rolled samples, respectively. It is seen from Fig. 3(a)

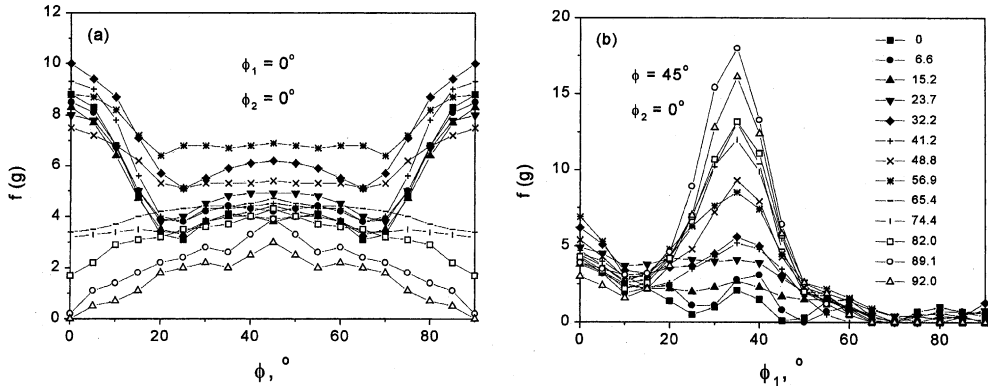


Fig. 3. Orientation intensity $f(g)$ along the line of (a) $\phi_1 = 0^\circ$ and (b) $\phi = 45^\circ$ at the plane of $\phi_2 = 0^\circ$ for different cold rolled samples after annealing at 371°C .

that the orientations similar to the cube orientation are within about 20° from the cube orientation at ϕ_1 and $\phi_2 = 0^\circ$, which is close to the value of 22.5° determined by Basson and Driver [6] based on the analysis of slip geometry. During cold rolling the cube orientation moves to the G orientation along the ϕ axis, and then moves to the B orientation. When the cold rolling reduction reaches about 90%, the intensity at the cube orientation decreases to 0, while the B orientation has a maximum intensity. The B orientation should be one of the arrival points of the cube orientation on the β fiber.

For the cube component, the distribution of intensities along the ϕ_1 axis is identical at different ϕ_2 planes. Fig. 4(a) and (b) show the intensities of the ODF $f(g)$ along the line of $\phi = 0^\circ$ and along the η fiber indicated in Fig. 2(b) at the plane of $\phi_2 = 45^\circ$ for different cold rolled samples. It is found in Fig. 4(a) that the rotated cube orientation is first rotated to the cube orientation so that the halfwidth (full width at half maximum) of the intensity peaks along the ϕ_1 axis decreases with increasing cold rolling reduction. It is seen in Fig. 4(b) that the cube orientation at ϕ_1 , ϕ , $\phi_2 = 0^\circ$, 45° , 45° is directly

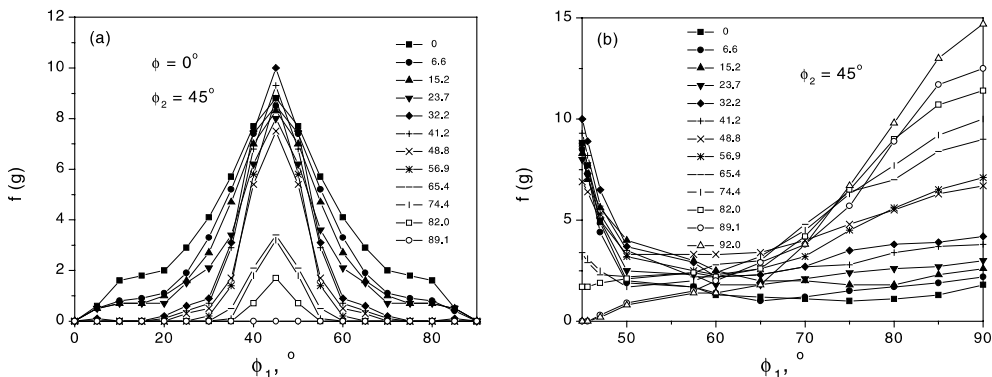


Fig. 4. Orientation intensity $f(g)$ along the line of $\phi = 0^\circ$ (a) and along the η fiber (b) at the plane of $\phi_2 = 45^\circ$ for different cold rolled samples.

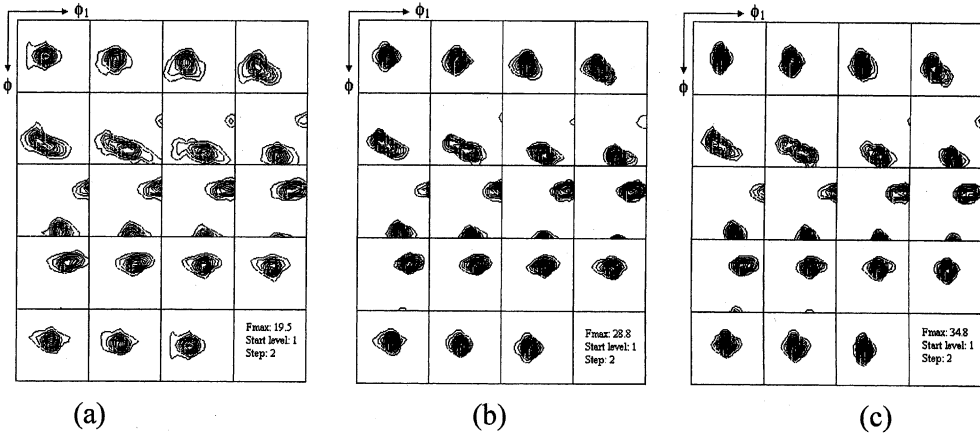


Fig. 5. ODFs of hot band samples cold rolled to reductions of (a) 0%, (b) 45.4%, and (c) 89.4%.

rotated to the D orientation along the η fiber. Similarly the cube orientations at $45^\circ < \phi_2 < 90^\circ$ are directly rotated to the positions between the B and D orientations on the β fiber.

Stability of the β fiber texture during cold rolling

Fig. 5 shows the ODFs of AA 5052 hot bands cold rolled to different reductions. A typical β fiber rolling texture has developed in the hot band, as shown in Fig. 5(a). The β fiber rolling texture and its center position in Euler space do not change during cold rolling. Fig. 6 shows the maximum intensities of the ODF $f(g)$ for a particular angle ϕ_2 along the β fiber of the resulting cold rolling texture. The intensity at the B orientation is still larger than that at the D orientation at large strains, which suggests that the B orientation does not rotate to the D orientation along the β fiber. This is different from

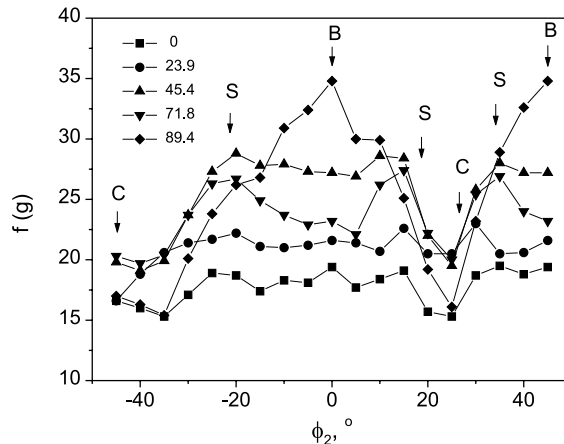


Fig. 6. Maximal intensity $f(g)$ for a particular angle ϕ_2 along the β fiber of the cold rolling texture for hot bands.

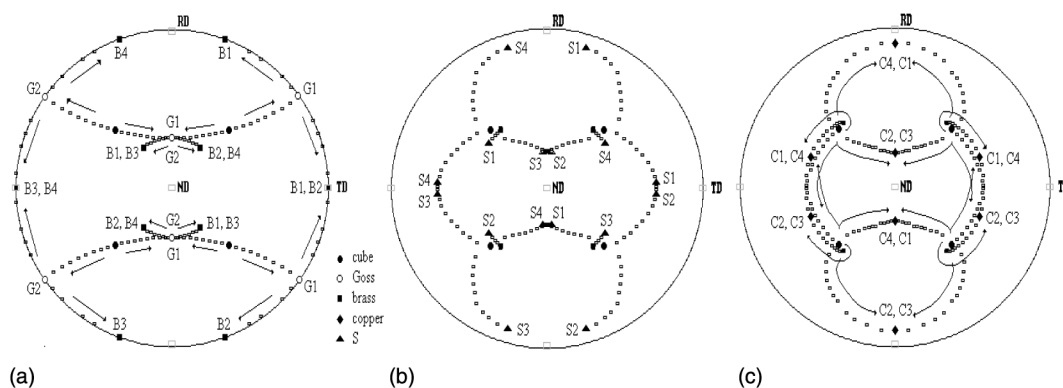


Fig. 7. Typical rotation paths from the cube orientation to the β fiber in $\{111\}$ pole figure.

the results predicted by using the Taylor RC-model [7] or a strain rate sensitivity model [8].

Discussion

Rotation of the cube orientation

The experimental results reveal that the cube oriented grains in a polycrystal aluminium alloy are rotated to the β fiber along different paths. Fig. 7 shows the typical rotation paths from the cube orientation to the β fiber in a $\{111\}$ pole figure. As shown in Fig. 7(a), the arrow first moves towards the G1 and G2 orientations in opposite directions, and then moves from the G1 orientation towards the B1 or B2 and from the G2 orientation towards the B3 or B4. This rotation path from the cube orientation to the B orientation is in agreement with the prediction made by using the N model [7], a strain rate sensitivity model [8] and a modified pencil glide theory [9]. The cube orientation can be directly rotated to the β fiber between the D (90, 30, 45) orientation and the B (35, 45, 90) orientation. For example, the cube orientation moves to the S and D orientations along the rotation paths indicated in Fig. 7(b) and (c). The rotation path from the cube orientation to the S orientation is close to the prediction by the Taylor RC-model [7]. In this model the (10, 0.1, 89.9) orientation moved at first towards the α fiber. It left the α fiber before reaching the B orientation and moved towards the S orientation, and finally reached the final stable positions at D or C.

Engler et al. [3] measured the $\{111\}$ pole figures of a cold rolled single crystal Al–1.8 wt.%Cu. In contrast to the rotation paths in Fig. 7, the variation in intensities with cold rolling reduction is located at the rotation path from the cube orientation to the S orientation. This indicates that the rotation path from the cube to the β fiber in polycrystalline materials is similar to that in single crystals.

Orientation stability

Stable orientations are defined as those which stay constant and towards which all neighboring orientations move during deformation. The cube component is converted

into the β fiber during rolling, which shows that the stable end orientation should be on the β fiber. If the C orientation is the stable end position, the B orientation rotates to the C orientation along the β fiber, leading to the increase of the intensity at the C orientation and the decrease of the intensity at the B orientation. However, it is seen from Fig. 6 that this situation does not occur when the hot bands with the β fiber rolling texture are cold rolled to 90%. Therefore, the β fiber can be inferred to be the stable end position.

The typical orientations on the β fiber are the B, S and C (or D) orientations. The stability of the B, S and D orientations has been reported in fcc single crystals. The B [10,11] and S [12] orientations exhibited a high degree of texture stability during rolling. The C oriented crystals rotated towards the D orientation in rolling [13] and channel die compression [14]. The D orientation remained stable up to high rolling strains in Al, while in Cu and Al–Cu it rotated back to the C orientation simultaneously with the formation of shear bands [13]. Obviously the stability of the B, S and D orientations in polycrystalline materials is in agreement with the results observed in single crystals.

Conclusions

The rotation path of the cube orientation during rolling was determined based on the variation in the orientation distribution function with reduction. The rotation path from the cube orientation to the β fiber can be divided into two cases. One case is that the cube orientation is rotated to the B orientation through the Goss orientation. In the other case the cube orientation is directly rotated to the β fiber between the D (90, 30, 45) orientation and the B (35, 45, 90) orientation. All the orientations on the β fiber are stable, and the B orientation does not rotate towards the D orientation during rolling.

References

- [1] Dillamore, I. L., & Katoh, H. (1974). *Met Sci* 8, 73.
- [2] Akef, A., & Driver, J. H. (1991). *Mater Sci Engng A* 132, 245.
- [3] Engler, O., Kong, X. W., & Lücke, K. H. (1999). *Scripta Mater* 41, 493.
- [4] Wert, J. A., Liu, Q., & Hansen, N. (1997). *Acta Mater* 45, 2565.
- [5] Liu, Q., Maurice, C., Driver, J. H., & Hansen, N. (1998). *Metall Trans A* 29A, 2333.
- [6] Basson, F., & Driver, J. H. (2000). *Acta Mater* 48, 2101.
- [7] Hirsch, J., & Lücke, K. (1988). *Acta Metall* 36, 2883.
- [8] Zhou, Y., Tóth, L. S., & Neale, K. W. (1992). *Acta Metall Mater* 40, 3179.
- [9] Masui, H. (1999). *Acta Mater* 47, 4283.
- [10] Malin, A., Huber, J., & Hatherly, M. (1981). *Z Metallk* 72, 310.
- [11] Godfrey, A., Juul Jensen, D., & Hansen, N. (1998). *Acta Mater* 46, 823.
- [12] Kamijo, T., Fujiwara, A., Yoneda, Y., & Fukutomi, H. (1991). *Acta Metall Mater* 39, 1947.
- [13] Wagner, P., Engler, O., & Lücke, K. (1995). *Acta Metall Mater* 43, 3799.
- [14] Godfrey, A., Juul Jensen, D., & Hansen, N. (1998). *Acta Mater* 46, 835.